HHS Public Access

Author manuscript

Free Radic Biol Med. Author manuscript; available in PMC 2017 February 14.

Published in final edited form as:

Free Radic Biol Med. 2017 January ; 102: 274–286. doi:10.1016/j.freeradbiomed.2016.11.046.

Cisplatin-induced mitochondrial dysfunction is associated with impaired cognitive function in rats

Naomi Lomeli[a], **Kaijun Di**[b,c], **Jennifer Czerniawski**[d,e], **John F. Guzowski**[d,e], and **Daniela A. Bota**[a,b,c,f,*]

[a]Department of Pathology & Laboratory Medicine, University of California Irvine, Irvine, CA, USA

[b]Department of Neurological Surgery, University of California Irvine, Irvine, CA, USA

[c]Chao Family Comprehensive Cancer Center, University of California Irvine, Irvine, CA, USA

[d]Department of Neurobiology & Behavior, University of California Irvine, Irvine, CA, USA

[e]Center for the Neurobiology of Learning & Memory, University of California Irvine, Irvine, CA, USA

[f]Department of Neurology, University of California Irvine, Irvine, CA, USA

Abstract

Purpose—Chemotherapy-related cognitive impairment (CRCI) is commonly reported following the administration of chemotherapeutic agents and comprises a wide variety of neurological problems. No effective treatments for CRCI are currently available. Here we examined the mechanisms involving cisplatin-induced hippocampal damage following cisplatin administration in a rat model and in cultured rat hippocampal neurons and neural stem/progenitor cells (NSCs). We also assessed the protective effects of the antioxidant, N-acetylcysteine in mitigating these damages.

Experimental design—Adult male rats received 6 mg/kg cisplatin in the acute studies. In chronic studies, rats received 5 mg/kg cisplatin or saline injections once per week for 4 weeks. N-acetylcysteine (250 mg/kg/day) or saline was administered for five consecutive days during cisplatin treatment. Cognitive testing was performed 5 weeks after treatment cessation. Cisplatin-treated cultured hippocampal neurons and NSCs were examined for changes in mitochondrial function, oxidative stress production, caspase-9 activation, and neuronal dendritic spine density.

Results—Acute cisplatin treatment reduced dendritic branching and spine density, and induced mitochondrial degradation. Rats receiving the chronic cisplatin regimen showed impaired performance in contextual fear conditioning, context object discrimination, and novel object recognition tasks compared to controls. Cisplatin induced mitochondrial DNA damage, impaired respiratory activity, increased oxidative stress, and activated caspase-9 in cultured hippocampal

*Corresponding author at: University of California Irvine, Sprague Hall B200, Irvine, CA, 92697, USA. dbota@uci.edu (D.A. Bota). . nrlomeli@uci.edu (N. Lomeli), kdi@uci.edu (K. Di), jczernia@uci.edu (J. Czerniawski), john.g@uci.edu (J.F. Guzowski)

Disclosure of potential conflicts of interest

The authors do not have any potential conflicts of interest to disclose.

Appendix A. Supporting information

Supplementary data associated with this article can be found in the online version at doi:10.1016/j.freeradbiomed.2016.11.046.

neurons and NSCs. N-acetylcysteine treatment prevented free radical production, ameliorated apoptotic cellular death and dendritic spine loss, and partially reversed the cisplatin-induced cognitive impairments.

Conclusions—Our results suggest that mitochondrial dysfunction and increased oxidative stress are involved in cisplatin-induced cognitive impairments. Therapeutic agents, such as N-acetylcysteine, may be effective in mitigating the deleterious effects of cisplatin.

Keywords

Cisplatin (CDDP); Chemotherapy; Neural stem/precursor cells (NSCs); Hippocampal neurons; N-acetylcysteine (NAC); Mitochondria; DNA damage; Oxidative stress; Chemotherapy-related cognitive impairment (CRCI)

1. Introduction

Chemotherapy causes short-term memory loss and concentration difficulties, which severely diminishes quality of life. Chemotherapy-related cognitive impairment (CRCI) encompasses a broad range of neurological problems, such as impairments in memory, attention, clarity of thought, executive functioning, and information processing speed [1,2]. CRCI is an ever-increasing problem of great clinical concern, up to 34% of patients experience persistent cognitive problems years after completing chemotherapy [3]. The underlying mechanisms of CRCI are not well understood, and no effective treatments are currently available.

Cisplatin (CDDP) is one of the most widely used cancer drugs; it is used to treat advanced ovarian and testicular cancer among other malignancies. CDDP can cross through the blood-brain barrier, and accumulates in the hippocampus [4,5]. CDDP is a DNA targeting agent, forming toxic platinum DNA adducts, inducing DNA damage and apoptosis [6]. In addition, CDDP forms adducts with mitochondrial DNA (*mt*DNA) and inhibits *mt*DNA replication and mitochondrial gene transcription [7,8]. Unlike nuclear DNA, mitochondria lack nucleotide excision repair mechanisms for *mt*DNA [9]. Studies examining the mechanisms of CDDP-induced peripheral neuropathy in dorsal root ganglion neurons and ototoxicity in the cochlea show that CDDP induces *mt*DNA damage and generation of reactive oxygen species, resulting in these two dose-limiting toxicities associated with CDDP treatment [9–11].

Ovarian cancer patients treated with CDDP consistently develop CRCI during and after platinum-based chemotherapy [12]. For example, when Hess et al. examined advanced ovarian cancer patients in detailed neuro-cognitive tests; impairment was detected in two or more cognitive domains in 40% of CDDP chemotherapy recipients [13]. The effects of CDDP on neural *mt*DNA could produce mitochondrial dysfunction and prolonged neurotoxicity after cessation of CDDP treatment, which may play a causal role in the development of CRCI [14,15]. We previously reported that at doses lower than those found in chemotherapy patients, CDDP can potentially induce both severe hippocampal synaptic damage and neural cell loss [16]. *In-vitro*, low-doses of CDDP (2 μM) kill 50% of human NSCs, while a dose five times higher (10 μM) is required to kill 50% of patient-derived malignant glioma stem-like cells [17]. To uncover the potential mechanisms underlying

CDDP-induced brain dysfunction we evaluated the effects of acute and chronic CDDP treatment at clinically relevant doses. We assessed cognitive changes using behavioral paradigms that engage the hippocampus. To evaluate the hypothesis that hippocampal mitochondrial dysfunction and oxidative stress may play a role in the development of CRCI, we examined the *in-vivo* effects of CDDP treatment on hippocampal neuronal dendritic complexity, mitochondrial integrity, and cellular death at several time-points after the cessation of treatment, as well as the *in-vitro* effects using cultured rat hippocampal neurons and NSCs. We also studied the effects of a clinically-available antioxidant, N-acetylcysteine (NAC) on mitigating CDDP-induced dendritic spine loss, oxidative stress, apoptosis, and cognitive dysfunction.

2. Materials and methods

2.1. Animals

Animal studies were performed in accordance with the guidelines established by the Institutional Animal Care and Use Committee (IACUC) of the University of California, Irvine. All the data were generated using Sprague Dawley rats (Charles River Laboratories). Experiments were approved by IACUC and conformed to NIH guidelines.

2.2. Drug treatments

Seventy-nine adult male Sprague Dawley rats weighing 200–250 g at the time of arrival served as subjects. For acute CDDP studies, rats were injected intraperitoneally with CDDP (Teva Pharmaceuticals USA, Inc.) dissolved in 0.9% saline (3 mg/kg/day) for 2 consecutive days (n=6). The control animals received 0.9% sterile saline of the same volume (n=6). For the chronic CDDP+NAC studies, rats received one CDDP (5 mg/kg, i.p.) or saline injection per week for four consecutive weeks. NAC (Cumberland Pharmaceuticals, 250 mg/kg/day, i.p.) was administered for five days starting two days before each CDDP administration and ending 2 days after the last dose of CDDP. On days of CDDP administration, NAC was given 4 h after CDDP injection. The rats were divided into four groups: saline-treated controls (Saline, n=25), N-acetylcysteine-treated (NAC, n=18), cisplatin-treated (CDDP, n=15), and cisplatin+N-acetylcysteine-treated (CDDP+NAC, n=13). Mannitol (APP Pharmaceuticals, 250 mg/kg, i.p.) was administered to all animals 1 h prior to CDDP, to minimize renal toxicity and increase diuresis. For the *in-vitro* NAC studies, NAC (Sigma) was added to the culture medium 30 min after CDDP treatment.

2.3. Golgi-Cox staining

Brains were harvested and subjected to Golgi-Cox impregnation as specified by the manufacturer's instructions (FD Rapid GolgiStain Kit, FD NeuroTechnologies, Inc). Coronal sections (200 μm) through the hippocampus were processed using Fluoromount G (Southern Biotech) mounting medium. Individual Golgi-impregnated CA3 pyramidal neurons were reconstructed and the dendritic branching and spines were quantified across the distance from the soma. Sholl analysis used a series of concentric circles (20 μm apart) to calculate the number of dendritic intersections as a function of distance from the soma.

2.4. Transmission Electron Microscopy (TEM)

Hippocampi were isolated from Sprague Dawley rats and fixed in glutaraldehyde. Hippocampal sections of the CA3 region were sent to the University of California, Irvine Health Research Services Core Facility for TEM processing and imaging.

2.5. Terminal deoxynucleotidyl transferase-mediated biotinylated UTP nick end labeling (TUNEL) Assay

Rats were sacrificed, and brains were harvested following 0.9% saline perfusion. Brains were rapidly removed, and flash frozen in isopentane and stored at −80 °C. Coronal sections (30 μm) through the hippocampus were processed for TUNEL assay. The TUNEL assay was performed using the NeuroTACS™ In Situ Apoptosis Detection Kit according to the manufacturer's instructions (Trevigen Inc).

2.6. Cognitive testing

Fear conditioning (FC), Context Object Discrimination (COD), and Novel Object Recognition (NOR) were done as previously published by JC and JG [18,19]. Cognitive testing was administered 5–6 weeks after the final and forth CDDP or saline injection. The experiment was repeated three times with three animal cohorts, and data from all three experiments were combined and shown in the results section. Detailed description is included in the Suppl. Data.

2.6.1. Fear conditioning—Rats were placed in a chamber for 5 min (baseline), followed by 5 tone (90db, 2000 Hz, 30 s) - shock (1 mA, 1 s) pairings over 5 min, and left in the conditioning chamber for an additional 5 min (post-training). The following day, rats were returned to the conditioning chamber for 5 min with no tone or shock presentations in order to assess conditioned freezing to the context (context test). The cue test was administered 1 h later, during which rats were placed in a novel context for 1 min (pre-cue test) followed by a 3 min tone presentation (cue test) and an additional 1 min (post-cue test). For training and testing, freezing behavior was scored as % time spent freezing, defined as complete immobility with the exception of breathing movements.

2.6.2. Context object discrimination—Rats were exposed to 2 different environments (termed A and B), located in adjacent rooms, for 5 min each per day for 2 consecutive days and allowed to freely explore [19]. Rats were returned to their home cage for a 20 min interval between training sessions. The order of context presentation was counterbalanced between subjects and across days. Each environment had 2 identical local objects (unique to each environment). On the third day, rats were tested in environment A for 5 min, in which one of the objects from B replaced one of the objects from A. Total exploration time, time spent exploring each object, and the discrimination ratio (time spent exploring the out-of-context object/total exploration time) were quantified.

2.6.3. Novel object recognition—Rats were placed in an open Plexiglas box arena (60×60 cm) with 60 cm high walls containing two identical objects. Each rat explored the arena for 5 min per day for 2 consecutive days. The 5 min test trial was given 24 h later, during which the rat was presented with one of the familiar objects paired with a novel

object. Total exploration time, time spent exploring each object, and the discrimination ratio (time spent exploring the novel object/total exploration time) were quantified.

2.7. Dissociated hippocampal neuron and NSC cultures

NSCs were isolated from the hippocampi of embryonic day 19 (E19) Sprague Dawley rats and cultured as previously described [16]. Passage 6–10 NSCs were used for experiments. Hippocampal neuron cultures were prepared from postnatal day 0 (P0) Sprague Dawley pups as previously described by our lab and others [16,20]. Neurons were used for experiments on 17–21 days *in-vitro* (17–21 DIV).

2.8. MitoTracker Red and immunocytochemistry

Neurons and NSCs were plated on 12 mm coverslips. NSCs were incubated in culture medium containing 500 nM Mitotracker Red CMXRos (Life Technologies) for 30 min at 37 °C and 5% CO_2. After incubation, cells were fixed with ice-cold 4% paraformaldehyde (PFA) in PBS, pH 7.4, for 12 min. NSCs were incubated in blocking buffer (0.2% Triton-X, 10% BSA in PBS, pH 7.4) for 1 h at room temperature. Rabbit anti-Caspase-9 (Cell Signaling) was diluted 1:50 for NSCs, and 1:200 in blocking buffer (0.1% Triton-X, 3% FBS in PBS, pH 7.4) for neurons overnight at 4 °C. Mouse anti-PSD95 1:2000 (Thermo Fisher) was used to visualize dendritic spines. The next day, coverslips were washed and incubated in the appropriate secondary antibodies conjugated to Alexa Fluor 488 at 1:200, or Alexa Fluor 594 at 1:400 (Invitrogen); at room temperature for 1.5 h. Cells were processed for imaging with DAPI Fluoromount G (Southern Biotech) mounting medium. Fluorescent images were generated using the Nikon Ti-E inverted microscope with a 20× objective (NA 0.75).

2.9. Measurement of oxidative stress

Neurons and NSCs plated on 12 mm coverslips were incubated in culture medium containing 5 μM Cell ROX Green Reagent (Life Technologies) for 20 min at 37 °C and 5% CO_2. After incubation, cells were fixed with ice-cold 4% PFA in PBS, pH 7.4 for 12 min, and washed with PBS before mounting. Cells were processed for imaging with DAPI Fluoromount G mounting medium. Neuronal images were generated using confocal microscopy, Zeiss LSM 700. 10 μm z-series (2 μm steps) images were captured at 20× (NA 0.8) spanning across entire neurons. NSC images were generated with an Olympus Scanner VS110 based on a BX61VS upright microscope with a 20× apochromatic objective (NA 0.75). Relative fluorescence intensity of CellROX green probe was quantified by ImageJ. Each experiment was repeated at least twice, with similar results. Each experiment included 3–4 sister coverslips per treatment group. For CellROX green fluorescence measurement, 5 frames were analyzed per coverslip, for a total of 150–200 cells per treatment group.

2.10. MtDNA qPCR assay

Total DNA was purified from cell samples using the Qiagen Genomic Tip and Genomic DNA Buffer Set Kit (Qiagen, Valencia, CA, USA). A mitochondrial fragment (235 bp) was amplified and standardized to a 12.5 Kb fragment from the nuclear encoded gene, Clusterin (*TRPM-2*). PCR products were normalized to control levels [21]. The sequences for rat

TRPM-2, *mt*DNA fragment (235 bp) primer sets were: *TRPM*-2 forward 5′-AGACGGGTGAGACAGCTGCACCTTTTC-3′, reverse 5-CGAGAGCATCAAGTGCAGGCATTAGAG-3′; *mt*DNA fragment forward 5′-CCTCCCATTCATTATCGCCGCCCTTGC-3′, reverse 5′-GTCTGGGTCTCCTAGTAGGTCTGGGAA-3′.

2.11. Quantitative RT-PCR assay

Total RNA was extracted using RNeasy Mini Kit (Qiagen) and cDNA was generated using the iScript™ cDNA Synthesis Kit (Bio-Rad). Quantitative PCR reactions (iQ™ SYBR Green Sumpermix, Bio-Rad) were conducted using a Bio-Rad CFX96 Real-time System, and the gene expression levels were normalized to those of *18S rRNA*. The sequences for rat *Cytochrome B* and *18S rRNA* primer sets were: *Cytochrome B* forward 5′-CGAAAATCTACCCCCTATT-3′, reverse 5′-GTGTTCTACTGGTTGGCCTC-3′; 18S *rRNA* forward 5′-TCAATCTCGGGTGGCTGAACG-3′, reverse 5′-GGACCAGAGCGAAAGCATTTG-3′. All primers were ordered from IDT, Integrated Device Technology, Inc, Coralville, Iowa, USA.

2.12. Seahorse XF24 metabolic flux analysis

Mitochondrial respiratory function was assessed using the Seahorse XF24 Extracellular Flux Analyzer. Oxygen consumption rates (OCR) were measured in adherent hippocampal neurons and NSCs using the Cell Mito Stress Kit [22,23] (Seahorse Bioscience). Dissociated hippocampal neurons from P0 pups were plated at a density of 7.5×10^4 cells/well in poly-D-lysine coated XF24 cell culture microplates. On the day of metabolic flux analysis, the neuronal culture medium was replaced with 500 µl of bicarbonate-free XF Base Medium (Seahorse Biosciences) supplemented with 17.5 mM glucose, and 0.23 mM sodium pyruvate, pH 7.4. Cells were washed once and incubated at 37 °C in a non-CO_2 incubator for 1 h. Baseline rates were measured at 37 °C three times before the sequential injection of the following mitochondrial inhibitors: oligomycin (2 µM), FCCP (1 µM), and lastly, rotenone (1 µM) and antimycin A (1 µM). NSCs (6×10^4 cells/well) were seeded in XF24 cell culture microplates pre-coated with fibronectin. The inhibitor concentrations used were oligomycin (1 µM), FCCP (2 µM), rotenone (1 µM), and antimycin A (1 µM). Three measurements were taken after addition of each inhibitor. All measurements were normalized to protein content per well using a Qubit 2.0 fluorometer (Invitrogen). Data was analyzed using Student's paired *t*-test. Data was graphed as mean ± SEM, n=3 per treatment group.

2.13. Systematic analysis and statistical considerations

Graphs and statistical analyses were prepared using GraphPad Prism 5.0 Software (GraphPad Software, La Jolla, CA, USA). Results are expressed as mean ± SEM. Comparison between control and treatment cohorts were made by unpaired Student's *t*-test, one-way ANOVA, or two-way repeated measures (RM) ANOVA. Statistical significance levels were set at 0.05. *Post hoc* analysis was made by Bonferroni correction.

3. Results

3.1. Acute cisplatin treatment produces long-term reduction in dendritic branching and spine density of hippocampal pyramidal neurons

Previously, we demonstrated that high-dose (20 mg/kg), acute CDDP exposure produces changes in hippocampal dendritic morphology of Sprague Dawley rats 3 days after treatment [16]. To study the long term effects of low-dose CDDP on dendritic morphology, adult Sprague Dawley rats were given a 6 mg/kg CDDP regimen administered over two consecutive days (3 mg/kg/day). We assessed dendritic branching (Fig. 1A, B) and spine density (Fig. 1C, D) at 14 and 28 days after treatment. This type of treatment directly translates to 18 mg/m^2/day in humans [24] – which is a lower dose than the lowest regimen administered to cancer patients, which is 50 mg/m^2 every three weeks [25]. Golgi-Cox impregnated neurons in the CA3 region revealed pronounced changes in dendritic morphology at 14 and 28 days after CDDP treatment. At 6 mg/kg, CDDP significantly reduced the dendritic branching of pyramidal neurons ($F_{(24,429)}$ =2.958, $P < 0.0001$) compared to controls (Fig. 1B). In addition, CDDP reduced the number of dendritic spines at 28 days after treatment cessation ($P < 0.0001$) (Fig. 1D).

3.2. Acute cisplatin treatment disrupts hippocampal mitochondrial morphology

CDDP accumulates in mitochondria and forms adducts with *mt*DNA and proteins [8,9]. To investigate the effect of CDDP on mitochondria of CA3 neurons, we assessed mitochondrial changes at 14 days and 28 days after CDDP administration (6 mg/kg) by TEM (Fig. 2). CA3 neurons from control rats showed intact normal mitochondria (Fig. 2A, D). Mitochondrial degradation and vacuolization was evident following 14 days (Fig. 2B, E) with more extensive damage seen at 28 days (Fig. 2C, F) after CDDP treatment.

3.3. Chronic cisplatin regimen impairs cognitive performance that is mitigated by treatment with N-acetylcysteine

3.3.1. Fear conditioning—To evaluate the effect of chronic CDDP administration on cognitive performance modeled on the clinical CDDP regimen, rats received one CDDP injection (5 mg/kg, intraperitoneal) per week for four consecutive weeks. NAC (250 mg/kg/day) was administered for five days starting two days before each CDDP cycle and ending two days after the last dose of CDDP. On days of CDDP administration, NAC was given 4 h after CDDP. Four hours was considered the optimal time to achieve NAC protection, without diminishing-anti-tumor efficacy in pediatric tumor models [26].

Cognitive performance in three tasks, fear conditioning (FC), context-object discrimination (COD), and novel object recognition (NOR) was assessed between five and six weeks after treatment discontinuation (Fig. 3A). Five weeks after the last CDDP injection, animals were tested on the FC task (Fig. 3B). Repeated measures (RM) two-way ANOVA revealed a main effect of testing phase ($F_{(4,252)}$ =550.6, $P < 0.0001$) and treatment group by phase interaction ($F_{(12,252)}$ =3.016, P=0.0006), and a main effect for treatment group ($F_{(3, 252)}$ =3.044, P=0.0352) for the percent time spent freezing during the FC task. During the context-test phase, CDDP animals spent significantly decreased percentages of time freezing compared with the control animals (*post hoc*, P=0.0018). Groups did not differ significantly in the

freezing behavior across baseline (P=0.984), post-training (P=0.6827), pre-cue (P=0.690), and cue test (P=0.320), indicating a selective deficit on the hippocampus-dependent contextual memory phase of the task. Administration of NAC prevented this CDDP-induced deficit. The CDDP group spent significantly less time freezing during the context test than the CDDP+NAC group (P=0.0005), whereas the saline control and CDDP+NAC groups did not differ (P=0.3213). All groups showed significant increases in freezing behavior after the tone-shock pairings (post-training phase) indicating that CDDP did not impair sensory perception. CDDP+NAC animals spent more time freezing during the cue-test compared with controls (P=0.0032). Cued-memory was intact in all groups; groups froze in response to 5 tone-shock pairings, which indicates that the CDDP-induced deficit was specific to memory of the context in which the pairing was learned.

3.3.2. Context object discrimination—After FC testing, animals were habituated and subjected to the COD task. There were no group differences in total time spent exploring objects (Suppl Fig. 2A), indicating that CDDP did not impair locomotor activity or exploratory motivation. While saline controls spent significantly more time exploring the out-of context object compared to the in-context object (P=0.0002), the CDDP-treated rats displayed no preference in exploring either object (P=0.8445) (Suppl Fig. 2B). A one-way ANOVA revealed a significant overall group effect for the discrimination ratio to differ between the groups ($F_{(3,67)}$ =4.558, P=0.0058). The discrimination ratio was calculated as [(time spent exploring out-of context object) /(total exploration time)] for each subject, with 1 being the maximum time spent exploring the out-of context object and 0 being maximum time exploring the in-context object **(**Fig. 3**C)**. The discrimination ratios significantly differed between the saline and CDDP groups (P=0.0012); with a discrimination ratio of 0.45 for CDDP-treated rats, indicating no discrimination between the in-context and out-of context objects. CDDP treatment diminished the ability to distinguish a previously experienced object, which was placed in a different context. NAC administration partially mitigated the CDDP-induced deficit, the discrimination ratios between the saline and CDDP +NAC groups were not significantly different ($P > 0.05$).

3.3.3. Novel object recognition—Following COD, rats were tested on the NOR task. There was no difference in total exploration time between saline and CDDP-treated animals (Suppl Fig. 2C). While saline controls spent significantly more time exploring the novel object compared to the familiar object ($P < 0.0001$), the CDDP-treated rats showed no preference in exploring either object (P=0.2241) (Suppl Fig. 2D). A one-way ANOVA did not reveal a significant overall group effect for the discrimination ratio to differ between the groups ($F_{(3,67)}$ =2.207, P=0.089) (Fig. 3D). The discrimination ratios differed significantly between saline and CDDP subjects (P=0.01). The CDDP-treated group had a discrimination ratio of 0.503, which indicates no preference between the familiar and novel objects. CDDP treatment impaired the ability to recognize a novel object from a previously experienced familiar object. NAC administration partially mitigated the CDDP-induced deficit, the discrimination ratios between the saline and CDDP+NAC groups were not significantly different (P=0.371). Together, these data suggest that chronic CDDP treatment results in cognitive deficits, which can be lessened by NAC.

3.4. Chronic cisplatin treatment increases apoptotic cell death in the hippocampal regions CA3, CA1, and subgranular zone (SGZ) of the dentate gyrus and decreases neurogenesis, NAC administration reduces cisplatin-induced cell death in these regions

To examine the effect of chronic CDDP treatment on neural apoptosis in the hippocampus, TUNEL was performed to detect apoptotic cells in the CA3, CA1, and SGZ of the dentate gyrus after behavioral testing, six weeks after treatment completion (Fig. 4A). One-way ANOVA analysis revealed a main effect for treatment group in CA3 ($F_{(3,32)}$ =12.67, P < 0.0001), CA1 ($F_{(3,32)}$ =5.747, P=0.0033), and SGZ ($F_{(3,32)}$ =12.54, P < 0.0001). CDDP-treatment increased the number of TUNEL(+) (apoptotic) nuclei in the CA3 (P < 0.001), CA1 (P < 0.01), and SGZ (P < 0.001) as compared with the saline group. NAC administration significantly reduced the CDDP-induced apoptotic cell death in the CA3 (P < 0.01), CA1 (P < 0.05), and SGZ (P < 0.001) as compared to CDDP treatment alone (Bonferroni's Multiple Comparison Test). There was no significant difference in the amount of TUNEL(+) cells in all three regions between the CDDP+NAC group, saline, and NAC groups (P > 0.05) (Fig. 4B), suggesting NAC prevented CDDP-induced neural death in the hippocampus.

To examine the effect of acute CDDP (6 mg/kg) treatment on hippocampal neurogenesis, quantification of Sox2(+) cells in the SGZ of CDDP-treated rats revealed a decrease in the number of NSCs 14 days after treatment (P=0.0306), with a greater decrease 28 days after treatment (P=0.0097)(Suppl Fig. 1). This data suggests that at concentrations lower than the therapeutic doses, CDDP can induce NSC damage which may impair neurogenesis long after exposure.

3.5. Cisplatin inhibits mtDNA synthesis in cultured hippocampal neurons and NSCs

We previously identified hippocampal neurons as being more sensitive to CDDP treatment than NSCs [16]. Schematic (Fig. 5A) depicts our findings on the sensitivities of hippocampal neurons and NSCs to CDDP. A sub-lethal (0.1 μM) dose of CDDP destroys synapses located on neuronal dendritic spines, whereas 1 μM CDDP induces measurable alterations on neuronal morphology and cell death. In contrast, 2 μM is the minimum dose that induces measurable apoptosis in NSCs, with 6 μM reducing cell survival to approximately 40%. Based on these studies, we selected these doses to assess mitochondrial function in cultured hippocampal neurons and NSCs. Previous studies have shown that CDDP binds to *mt*DNA in mouse liver [27] and dorsal root ganglion neurons [9]. However, the effects of CDDP on hippocampal neuron and NSC *mt*DNA have not been investigated. *Mt*DNA is a 16.3 Kb circular piece of DNA that encodes for 13 proteins that are essential components of the electron transport chain. To investigate if CDDP affects *mt*DNA in hippocampal neurons and NSCs, we examined the direct effect of CDDP on *mt*DNA replication in these cells. We used a PCR based assay to amplify a *mt*DNA fragment, in which many DNA lesions block the Taq DNA polymerase progression, resulting in decreased amplification of the damaged DNA template. CDDP produced a time-dependent preferential decrease in amplification of neuronal *mt*DNA as compared with a nuclear gene (Clusterin) **(**Fig. 5**B)**. CDDP (1 μM) significantly reduced *mt*DNA amplification as early as 4 h post-treatment compared to control (P=0.0077). Further decreases in neuronal *mt*DNA

amplification were observed at 24 h (P=0.0007) and 48 h post-treatment (P=0.0002) compared to control.

CDDP produced a dose and time-dependent decrease in amplification of NSC *mt*DNA (Fig. 5C). CDDP (6 μM) significantly reduced *mt*DNA amplification at 4 h (P=0.0176) and 48 h (P=0.0232) post-treatment compared to control. CDDP (2 μM) produced a slight decrease in *mt*DNA amplification at 48 h, although not significant (P=0.2416).

3.6. Cisplatin inhibits mtRNA transcription in NSCs

To examine whether CDDP-induced *mt*DNA damage could affect the transcription of mitochondrial genes, we assessed the transcription of Cytochrome B (CytB) in NSCs following CDDP treatment. CytB is a major subunit of complex III of the mitochondrial electron transport chain, and is *mt*DNA encoded [28,29]. We assessed CytB transcription following CDDP treatment (2 μM, 6 μM) at 0, 2, 4, 48 h post-treatment (Fig. 5D). CDDP treatment resulted in a significant decrease in CytB RNA levels at 2 μM ($P < 0.0001$) and 6 μM ($P < 0.0001$) as early as 2 h post-treatment. This finding suggests that CDDP-induced *mt*DNA damage may result in changes in mitochondrial respiratory function.

3.7. Cisplatin reduces mitochondrial respiratory rates in cultured hippocampal neurons and NSCs

To investigate if CDDP affects mitochondrial respiratory activity in hippocampal neurons and NSCs, we measured oxygen consumption rates (OCR) in these cells following CDDP treatment using the Seahorse XF24 extracellular flux analyzer. OCR is a measurement of oxidative phosphorylation. We examined the effect of 0.1 μM CDDP on hippocampal neurons following 24 h, 48 h, and 7 days of treatment (Fig. 5E, F). Basal OCR was significantly reduced at 24 h ($P < 0.0001$) and 48 h ($P < 0.0001$) compared to untreated. Basal OCR levels 7 days after treatment remained significantly lower compared to untreated levels (P=0.0012). We also examined the effect of CDDP on hippocampal neurons at a higher dose, 1 μM, which significantly reduced basal OCR levels at 48 h ($P < 0.0001$) compared to untreated (Fig. 5G, H).

NSC mitochondrial respiratory rates were also affected by CDDP treatment. We examined the effect of 2 μM CDDP on NSCs following 24 h, 48 h, and 7 days of treatment (Fig. 5I, J). Basal OCR was significantly reduced at 24 h (P=0.0266) and 48 h (P=0.0127). Basal OCR levels increased 7 days after treatment back to control levels (P=0.2452). A pronounced decrease in basal OCR was seen following 24 h of CDDP (6 μM, P=0.0075). These results indicate that CDDP impairs mitochondrial respiratory function in hippocampal neurons and NSCs, which may be long-lasting.

3.8. Cisplatin-induced oxidative stress is attenuated by N-acetylcysteine in cultured hippocampal neurons and NSCs

Mitochondria are the main sources of cellular reactive oxygen species (ROS) production. Oxidative stress is involved in the pathogenesis of CDDP-induced dose-limiting toxicities, including nephrotoxicity [30], ototoxicity [31], and peripheral neuropathy [32]. We examined oxidative stress production in hippocampal neurons and NSCs following CDDP

treatment (Fig. 6). Cultured hippocampal neurons were treated with CDDP (0.1 μM, 1 μM) for 48 h. The neurons were then incubated with CellROX fluorescent probe for 20 min and ROS production was measured by fluorescence intensity analysis of confocal images (Fig. 6A). CDDP treatment significantly increased oxidative stress levels as quantified by relative fluorescence intensity at 0.1 μM ($P < 0.0117$) and 1 μM ($P < 0.0062$) compared to control (Fig. 6B). To further examine CDDP increases in mitochondria-generated ROS, we examined the effect of NAC on oxidative stress levels following CDDP treatment. Addition of NAC (2.5 mM) significantly reduced oxidative stress levels in neurons treated with 0.1 μM ($P < 0.0001$) and 1 μM ($P < 0.0001$). CDDP treatment significantly increased oxidative stress in NSCs at 2 μM ($P < 0.0001$) and 6 μM ($P < 0.001$) compared to control (Fig. 6C,D). NAC (5 mM) significantly mitigated oxidative stress levels in NSCs treated with 2 μM ($P < 0.001$) and 6 μM ($P < 0.001$).

3.9. N-acetylcysteine treatment mitigates cisplatin-induced neuronal dendritic spine loss

The effects of CDDP on neuronal respiratory dysfunction and increased oxidative stress suggested that mitochondrial damage might contribute to CDDP-induced spine loss. Previously, we showed that CDDP reduces post-synaptic density-95 (PSD95) puncta and dendritic spine density in a time- and dose-dependent manner [16]. To test this idea, neurons were treated with CDDP (1 μM) in the presence or absence of NAC (2.5 mM) (Fig. 7A), and analyzed by PSD95 immuno-labeled puncta 48 h after treatment (Fig. 7B). CDDP reduced the number of PSD95 puncta as compared with controls ($F_{(3,80)} = 11.71$, $P = 0.001$, n=12), and *post hoc* comparisons showed that NAC partially restored dendritic spine density at 40–100 μm. These results suggest that CDDP-induced dendritic spine loss involves mitochondrial dysfunction although other mechanisms could also play a role.

3.10. N-acetylcysteine treatment ameliorates cisplatin-induced apoptosis in hippocampal neurons and NSCs

Next, we sought to examine whether CDDP induced mitochondrially-mediated apoptosis in cultured hippocampal neurons and NSCs through caspase-9 activation, and if NAC could protect against caspase-9 activation. Caspase-9 is a member of the cysteine aspartic acid protease (caspase) family. Upon apoptotic stimulation, cytochrome c is released from the mitochondria and associates with procaspase/Apaf-1 [33]. Apaf-1 activates caspase-9 by cleaving it at Asp315. Cleaved caspase-9 further activates other caspase proteins to initiate a caspase cascade that culminates in apoptosis [34]. Hippocampal neurons were treated with CDDP (1 μM) in the presence or absence of NAC, and cleaved caspase-9 expression was quantified by fluorescence microscopy (Fig. 7C, D). CDDP (1 μM) increased the percentage of cleaved caspase-9 expressing neurons ($P < 0.0001$) compared to control levels. NAC decreased cleaved caspase-9 expression in CDDP+NAC treated neurons ($P < 0.0001$) as compared with CDDP treatment alone. Notably, the percentage of cleaved caspase-9 expressing neurons was not different between the control and CDDP+NAC groups ($P = 0.7570$). CDDP (6 μM) increased the percentage of cleaved caspase-9 expression in NSCs ($P < 0.0001$) compared to control (Fig. 7E, F). MitoTracker Red probe was used to label mitochondria in NSCs. NAC decreased cleaved caspase-9 expression in CDDP+NAC treated NSCs ($P < 0.0001$) as compared with CDDP treatment alone. Cleaved caspase-9

expression was not significantly different between the CDDP+NAC and control groups (P=0.0606).

4. Discussion

CDDP is the first platinum anti-cancer agent to be widely used in the treatment of several malignancies including lung, ovarian, testicular, and head and neck cancer [35–37]. CDDP interacts with DNA causing DNA-Pt adducts which result in DNA crosslinking and apoptosis. A neurological complication of CDDP chemotherapy is cognitive impairment; however the underlying mechanisms are not well understood. Here, we examine the mechanisms of CDDP-induced neurotoxicity by utilizing a rodent model to evaluate the effects of acute and chronic CDDP regimens on neuronal integrity and cognitive function. In addition, we used cultured rat hippocampal neurons and NSCs to elucidate the mitochondria-mediated mechanisms underlying the sensitivity of these cell populations to CDDP. We report that acute CDDP (6 mg/kg) treatment reduced hippocampal dendritic branching and spine density of CA3 pyramidal neurons. When examining mitochondria of CA3 hippocampal neurons by TEM, we found that acute CDDP induced mitochondrial degradation and vacuolization with loss of cristae. Extensive apoptosis was also observed in the CA1, CA3, and SGZ of the dentate gyrus in the hippocampus of rats treated with the chronic CDDP regimen, as quantified by TUNEL. Notably, the CDDP-induced apoptosis and cognitive impairments were attenuated by NAC administration, suggesting that oxidative stress may be involved in the mechanism of CDDP-induced cognitive impairments. CDDP may produce changes in the hippocampus that persist after the completion of chemotherapy treatment. CDDP kills vulnerable NSCs and neuronal populations, and those that do survive suffer extensive damage including mitochondrial dysfunction and oxidative stress.

Neuroimaging studies have reported structural and functional changes in the brain associated with chemotherapy [38]. Most of these studies focus on the breast cancer population, as this group commonly reports cognitive problems after chemotherapy. Magnetic resonance imaging (MRI) studies of breast cancer patients have found reduced hippocampal volume [39,40] and grey and white matter abnormalities [41,42]. Notably McDonald et al. reports prominent reductions in grey matter density in multiple brain regions including the hippocampus of breast cancer patients as early as one month after completion of chemotherapy with partial recovery one year later. These structural changes correlate with decreased episodic memory, working memory, and attention deficits – all symptoms of CRCI [43,44]. In addition, a prospective study examining the effects of CDDP in testicular cancer patients found widespread reductions in grey matter in multiple brain regions as well as a reduction in performance in neurocognitive testing six months after the completion of CDDP treatment [45].

Additional imaging and functional studies examining the neurological changes associated with CDDP chemotherapy in the cancer population are clearly warranted. However, studies examining platinum concentrations in the brains of patients that received CDDP chemotherapy for CNS [46] and non-CNS tumors [47] detected platinum (Pt) concentrations ranging between 0.33 and 2.9 μg/g. More recent studies have detected Pt in the brains of

rodents following chronic CDDP administration ranging between 0.1 and 2.4 μg/g [4,5]. Köppen et al. detected high concentrations of Pt (0.6–1.9 μg/g) in the hippocampus. Based on these studies, it is plausible that CDDP results in structural CNS changes that correlate with the cognitive deficits observed in CDDP-treated patients [12,13].

The decrease in the NSC population caused by NSC death and reduced hippocampal neurogenesis following chemotherapy treatment may prolong the regeneration of hippocampal neurons - which are critical for learning and memory processes. Impairment of hippocampal neurogenesis as well as NSC death following chemotherapy is linked to the cognitive and mood-based deficits observed in patients and animal models undergoing cancer therapies [48–50].

Due to the CDDP-induced damage to dendritic branching and spines, as well as apoptosis of neurons and NSCs within the hippocampal formation at the cellular level, it follows that cognitive tasks that require the hippocampus would be particularly vulnerable to CDDP at the behavioral level. To recapitulate the clinical regimen, rats received one weekly CDDP injection (5 mg/kg) or saline for four consecutive weeks, and performance on FC, COD, and NOR was assessed five to six weeks post-treatment. This five week interlude allowed animals to rest following chemotherapy to minimize sickness behavior affecting performance in testing, and allowed us to examine long-term effects of CDDP on cognitive performance. The CDDP group was impaired in the context but not cued FC; they spent significantly less time engaged in freezing behavior than saline controls during the context test of FC. No difference was observed in freezing behavior between CDDP and control groups during the cue-test, suggesting that CDDP selectively disrupted the memory for context-shock association, which requires intact hippocampal function, and not the CS-US association, which does not require the hippocampus. Moreover, CDDP-treated rats spent significantly less time exploring the out-of context object during the COD task. As the hippocampus is critical for both context fear conditioning and COD, these results suggest that CDDP disrupts hippocampal function which impairs context memory. Consistent with the notion, clinically, reduced hippocampal volume and neurogenesis loss have been found in chemotherapy treated colon cancer patients [51] and brain tumor patients [52]. However, CDDP-treated rats also failed to discriminate between the novel and familiar objects during NOR; the NOR task engages the medial prefrontal cortex and perirhinal cortex in addition to the hippocampus. This suggests that although CDDP impairs hippocampal function, additional regions may be affected.

In our search for mechanisms involving CDDP-induced cognitive decrements and neurotoxicity observed *in-vivo*, we found that CDDP induces *mt*DNA damage and impairs respiratory activity in cultured rat hippocampal neurons and NSCs. Mitochondrial dysfunction increases oxidative stress, which provokes free radical production, resulting in dendritic spine loss. Severe mitochondrial dysfunction promotes caspase-9 activation and apoptosis. We found that delayed NAC treatment prevented increases in oxidative stress; ameliorated caspase-9 activation in CDDP treated hippocampal neurons and NSCs, and partially mitigated neuronal dendritic spine loss. NAC administration during chronic CDDP regimen reduced the CDDP-induced cognitive deficits and ameliorated CDDP-induced apoptotic cell death in the hippocampus. These findings suggest that mitochondrial

dysfunction is a strong candidate mechanism for CDDP related cognitive impairments and neurotoxicity.

Oxidative stress and mitochondrial dysfunction in the brain have been associated with other chemotherapeutic agents that induce cognitive impairments, such as adriamycin and cyclophosphamide [53–55], and antioxidant intervention has shown to be a promising therapy in preventing CRCI [56,57]. NAC is a precursor of glutathione, the most important intracellular antioxidant [58]. NAC is able to cross the blood-brain barrier [59], and has proven efficacy in both human [60,61] and rodent models of neurodegenerative disorders [62]. In cancer patients, glutathione levels are severely reduced by CDDP treatment, while glutathione supplementation prevents oxidative damage caused by mitochondrial dysfunction [63]. Oral NAC was studied in multiple clinical trials in combination with CDDP and has shown some promising results in preventing CDDP-induced ototoxicity [31] and peripheral neuropathy [32]. NAC prevents cancer recurrence in colon cancer patients [64] and its addition to chemotherapy does not decrease the anti-cancer effect of other drugs [65,66]. Our data suggests that NAC lessens CDDP-induced cognitive deficits by preventing free radical production, and ameliorating hippocampal apoptotic neural death and dendritic spine loss.

By assessing the effects of CDDP administration on both cognition and neural damage, this study advances the understanding of mechanisms underlying CRCI.

Supplementary Material

Refer to Web version on PubMed Central for supplementary material.

Acknowledgements

We thank Dr. Kevin Kong of the University of California, Irvine Chao Family Comprehensive Cancer Center for advice and providing the pharmaceutical grade drugs used in our studies. We also thank Xing Gong for technical help with immunohistochemistry.

Financial support

This work was supported by the National Institute for Neurological Diseases and Stroke Award (NINDS/NIH) [NS072234], the National Center for Advancing Translational Sciences, NIH [UL1 TR001414], and the UCI Cancer Center Award [P30CA062203] from the National Cancer Institute. The NIH MBRS-IMSD training grant [GM055246] and the NINDS/NIH pre-doctoral fellowship [NS082174] provided support for N. Lomeli.

Abbreviations

CDDP	cisplatin
COD	context object discrimination
FC	fear conditioning
NAC	N-acetylcysteine
NOR	novel object recognition
NSCs	neural/stem progenitor cells

ROS	reactive oxygen species
TUNEL	terminal deoxynucleotidyl transferase (TdT) dUTP Nick-End Labeling

References

[1]. Argyriou AA, Assimakopoulos K, Iconomou G, Giannakopoulou F, Kalofonos HP. Either called "chemobrain" or "chemofog," the long-term chemotherapy-induced cognitive decline in cancer survivors is real. J. Pain. Symptom Manag. 2011; 41:126–139.

[2]. Weiss B. Chemobrain: a translational challenge for neurotoxicology. Neurotoxicology. 2008; 29:891–898. [PubMed: 18479752]

[3]. Ahles TA, Saykin AJ. Candidate mechanisms for chemotherapy-induced cognitive changes. Nat. Rev. Cancer. 2007; 7:192–201. [PubMed: 17318212]

[4]. Screnci D, McKeage MJ, Galettis P, Hambley TW, Palmer BD, Baguley BC. Relationships between hydrophobicity, reactivity, accumulation and peripheral nerve toxicity of a series of platinum drugs. Br. J. Cancer. 2000; 82:966–972. [PubMed: 10732773]

[5]. Koppen C, Reifschneider O, Castanheira I, Sperling M, Karst U, Ciarimboli G. Quantitative imaging of platinum based on laser ablation-inductively coupled plasma-mass spectrometry to investigate toxic side effects of cisplatin. Metallomics: Integr. Biometal Sci. 2015; 7:1595–1603.

[6]. Dzagnidze A, Katsarava Z, Makhalova J, et al. Repair capacity for platinum-DNA adducts determines the severity of cisplatin-induced peripheral neuropathy. J. Neurosci. 2007; 27:9451–9457. [PubMed: 17728458]

[7]. Todd RC, Lippard SJ. Inhibition of transcription by platinum antitumor compounds. Metallomics: Integr. Biometal Sci. 2009; 1:280–291.

[8]. Yang Z, Schumaker LM, Egorin MJ, Zuhowski EG, Guo Z, Cullen KJ. Cisplatin preferentially binds mitochondrial DNA and voltage-dependent anion channel protein in the mitochondrial membrane of head and neck squamous cell carcinoma: possible role in apoptosis. Clin. Cancer Res. 2006; 12:5817–5825. [PubMed: 17020989]

[9]. Podratz JL, Knight AM, Ta LE, et al. Cisplatin induced mitochondrial DNA damage in dorsal root ganglion neurons. Neurobiol. Dis. 2011; 41:661–668. [PubMed: 21145397]

[10]. Areti A, Yerra VG, Naidu V, Kumar A. Oxidative stress and nerve damage: role in chemotherapy induced peripheral neuropathy. Redox Biol. 2014; 2:289–295. [PubMed: 24494204]

[11]. Kim HJ, Lee JH, Kim SJ, et al. Roles of NADPH oxidases in cisplatin-induced reactive oxygen species generation and ototoxicity. J. Neurosci. 2010; 30:3933–3946. [PubMed: 20237264]

[12]. Correa DD, Hess LM. Cognitive function and quality of life in ovarian cancer. Gynecol. Oncol. 2012; 124:404–409. [PubMed: 22094932]

[13]. Hess LM, Chambers SK, Hatch K, et al. Pilot study of the prospective identification of changes in cognitive function during chemotherapy treatment for advanced ovarian cancer. J. Support Oncol. 2010; 8:252–258. [PubMed: 21265392]

[14]. Verstappen CC, Heimans JJ, Hoekman K, Postma TJ. Neurotoxic complications of chemotherapy in patients with cancer: clinical signs and optimal management. Drugs. 2003; 63:1549–1563. [PubMed: 12887262]

[15]. Schagen SB, Muller MJ, Boogerd W, Mellenbergh GJ, van Dam FS. Change in cognitive function after chemotherapy: a prospective longitudinal study in breast cancer patients. J. Natl. Cancer Inst. 2006; 98:1742–1745. [PubMed: 17148777]

[16]. Andres AL, Gong X, Di K, Bota DA. Low-doses of cisplatin injure hippocampal synapses: a mechanism for 'chemo' brain? Exp. Neurol. 2014; 255:137–144. [PubMed: 24594220]

[17]. Gong X, Schwartz PH, Linskey ME, Bota DA. Neural stem/progenitors and glioma stem-like cells have differential sensitivity to chemotherapy. Neurology. 2011; 76:1126–1134. [PubMed: 21346220]

[18]. Czerniawski J, Guzowski JF. Acute neuroinflammation impairs context discrimination memory and disrupts pattern separation processes in hippocampus. J. Neurosci. 2014; 34:12470–12480. [PubMed: 25209285]

[19]. Czerniawski J, Miyashita T, Lewandowski G, Guzowski JF. Systemic lipopolysaccharide administration impairs retrieval of context-object discrimination, but not spatial, memory: evidence for selective disruption of specific hippocampus-dependent memory functions during acute neuroinflammation. Brain Behav. Immun. 2015; 44:159–166. [PubMed: 25451612]

[20]. Andres AL, Regev L, Phi L, Seese RR, Chen Y, Gall CM, Baram TZ. NMDA receptor activation and calpain contribute to disruption of dendritic spines by the stress neuropeptide CRH. J. Neurosci. 2013; 33:16945–16960. [PubMed: 24155300]

[21]. Santos JH, Meyer JN, Mandavilli BS, Van Houten B. Quantitative PCR-based measurement of nuclear and mitochondrial DNA damage and repair in mammalian cells. Methods Mol. Biol. 2006; 314:183–199. [PubMed: 16673882]

[22]. Dranka BP, Benavides GA, Diers AR, et al. Assessing bioenergetic function in response to oxidative stress by metabolic profiling. Free Radic. Biol. Med. 2011; 51:1621–1635. [PubMed: 21872656]

[23]. Zhang J, Nuebel E, Wisidagama DR, Setoguchi K, et al. Measuring energy metabolism in cultured cells, including human pluripotent stem cells and differentiated cells. Nat. Protoc. 2012; 7:1068–1085. [PubMed: 22576106]

[24]. Reagan-Shaw S, Nihal M, Ahmad N. Dose translation from animal to human studies revisited. FASEB J. 2007; 22:659–661. [PubMed: 17942826]

[25]. Rene NJ, Cury FB, Souhami L. Conservative treatment of invasive bladder cancer. Curr. Oncol. 2009; 16:36–47.

[26]. Muldoon LL, Wu YJ, Pagel MA, Neuwelt EA. N-acetylcysteine chemoprotection without decreased cisplatin antitumor efficacy in pediatric tumor models. J. Neurooncol. 2015; 121:433–440. [PubMed: 25411097]

[27]. Rosen M, Figliomeni M, Simpkins H. The interaction of platinum antitumour drugs with mouse liver mitochondria. Int. J. Exp. Pathol. 1992; 73:61–74. [PubMed: 1315566]

[28]. Clayton DA. Replication and transcription of vertebrate mitochondrial DNA. Annu. Rev. Cell Biol. 1991; 7:453–478. [PubMed: 1809353]

[29]. Asin-Cayuela J, Gustafsson CM. Mitochondrial transcription and its regulation in mammalian cells. Trends Biochem. Sci. 2007; 32:111–117. [PubMed: 17291767]

[30]. Latcha S, Jaimes EA, Patil S, Glezerman IG, Mehta S, Flombaum CD. Long-term renal outcomes after cisplatin treatment. Clin. J. Am. Soc. Nephrol. 2016; 11:1173–1179. [PubMed: 27073199]

[31]. Yoo J, Hamilton SJ, Angel D, et al. Cisplatin otoprotection using transtympanic L-N-acetylcysteine: a pilot randomized study in head and neck cancer patients. Laryngoscope. 2014; 124:E87–E94. [PubMed: 23946126]

[32]. Lin PC, Lee MY, Wang WS, et al. N-acetylcysteine has neuroprotective effects against oxaliplatin-based adjuvant chemotherapy in colon cancer patients: preliminary data. Support Care Cancer. 2006; 14:484–487. [PubMed: 16450089]

[33]. Kuwahara D, Tsutsumi K, Kobayashi T, Hasunuma T, Nishioka K. Caspase-9 regulates cisplatin-induced apoptosis in human head and neck squamous cell carcinoma cells. Cancer Lett. 2000; 148:65–71. [PubMed: 10680594]

[34]. Jiang X, Wang X. Cytochrome c promotes caspase-9 activation by inducing nucleotide binding to Apaf-1. J. Biol. Chem. 2000; 275:31199–31203. [PubMed: 10940292]

[35]. Dasari S, Tchounwou PB. Cisplatin in cancer therapy: molecular mechanisms of action. Eur. J. Pharmacol. 2014; 740:364–378. [PubMed: 25058905]

[36]. Jamieson ER, Lippard SJ. Structure, recognition, and processing of cisplatin-DNA adducts. Chem. Rev. 1999; 99:2467–2498. [PubMed: 11749487]

[37]. Florea AM, Busselberg D. Cisplatin as an anti-tumor drug: cellular mechanisms of activity, drug resistance and induced side effects. Cancers. 2011; 3:1351–1371. [PubMed: 24212665]

[38]. Saykin AJ, Ahles TA, McDonald BC. Mechanisms of chemotherapy-induced cognitive disorders: neuropsychological, pathophysiological, and neuroimaging perspectives. Semin. Clin. Neuropsychiatry. 2003; 8:201–216. [PubMed: 14613048]

[39]. Kesler S, Janelsins M, Koovakkattu D, et al. Reduced hippocampal volume and verbal memory performance associated with interleukin-6 and tumor necrosis factor-alpha levels in

chemotherapy-treated breast cancer survivors. Brain Behav. Immun. 2013; 30(Suppl.):S109–S116. [PubMed: 22698992]

[40]. Bergouignan L, Lefranc JP, Chupin M, Morel N, Spano JP, Fossati P. Breast cancer affects both the hippocampus volume and the episodic autobiographical memory retrieval. PLoS One. 2011; 6:e25349. [PubMed: 22016764]

[41]. de Ruiter MB, Reneman L, Boogerd W, et al. Late effects of high-dose adjuvant chemotherapy on white and gray matter in breast cancer survivors: converging results from multimodal magnetic resonance imaging. Hum. Brain Mapp. 2012; 33:2971–2983. [PubMed: 22095746]

[42]. McDonald BC, Conroy SK, Ahles TA, West JD, Saykin AJ. Gray matter reduction associated with systemic chemotherapy for breast cancer: a prospective MRI study. Breast Cancer Res. Treat. 2010; 123:819–828. [PubMed: 20690040]

[43]. Kam JW, Boyd LA, Hsu CL, et al. Altered neural activation during prepotent response inhibition in breast cancer survivors treated with chemotherapy: an fMRI study. Brain Imaging Behav. 2016; 10:840–848. [PubMed: 26489975]

[44]. Kam JW, Brenner CA, Handy TC, et al. Sustained attention abnormalities in breast cancer survivors with cognitive deficits post chemotherapy: an electrophysiological study. Clin. Neurophysiol. 2016; 127:369–378. [PubMed: 25868929]

[45]. Amidi A, Agerbaek M, Wu LM, et al. Changes in cognitive functions and cerebral grey matter and their associations with inflammatory markers, endocrine markers, and APOE genotypes in testicular cancer patients undergoing treatment. Brain Imaging Behav. 2016

[46]. Stewart DJ, Leavens M, Maor M, et al. Human central nervous system distribution of cis-diamminedichloroplatinum and use as a radiosensitizer in malignant brain tumors. Cancer Res. 1982; 42:2474–2479. [PubMed: 6280860]

[47]. Gregg RW, Molepo JM, Monpetit VJ, et al. Cisplatin neurotoxicity: the relationship between dosage, time, and platinum concentration in neurologic tissues, and morphologic evidence of toxicity. J. Clin. Oncol. 1992; 10:795–803. [PubMed: 1569451]

[48]. Pereira Dias G, Hollywood R, Bevilaqua MC, et al. Consequences of cancer treatments on adult hippocampal neurogenesis: implications for cognitive function and depressive symptoms. Neuro Oncol. 2014; 16:476–492. [PubMed: 24470543]

[49]. Dietrich J, Han R, Yang Y, Mayer-Proschel M, Noble M. CNS progenitor cells and oligodendrocytes are targets of chemotherapeutic agents in vitro and in vivo. J. Biol. 2006; 5:22. [PubMed: 17125495]

[50]. Seigers R, Fardell JE. Neurobiological basis of chemotherapy-induced cognitive impairment: a review of rodent research. Neurosci. Biobehav. Rev. 2011; 35:729–741. [PubMed: 20869395]

[51]. Schneiderman B. Hippocampal volumes smaller in chemotherapy patients. Lancet Oncol. 2004; 5:202. [PubMed: 15085849]

[52]. Monje ML, Vogel H, Masek M, Ligon KL, Fisher PG, Palmer TD. Impaired human hippocampal neurogenesis after treatment for central nervous system malignancies. Ann. Neurol. 2007; 62:515–520. [PubMed: 17786983]

[53]. Joshi G, Aluise CD, Cole MP, et al. Alterations in brain antioxidant enzymes and redox proteomic identification of oxidized brain proteins induced by the anti-cancer drug adriamycin: implications for oxidative stress-mediated chemobrain. Neuroscience. 2010; 166:796–807. [PubMed: 20096337]

[54]. Joshi G, Sultana R, Tangpong J, et al. Free radical mediated oxidative stress and toxic side effects in brain induced by the anti cancer drug adriamycin: insight into chemobrain. Free Radic. Res. 2005; 39:1147–1154. [PubMed: 16298740]

[55]. Konat GW, Kraszpulski M, James I, Zhang HT, Abraham J. Cognitive dysfunction induced by chronic administration of common cancer chemotherapeutics in rats. Metab. Brain Dis. 2008; 23:325–333. [PubMed: 18690526]

[56]. Joshi G, Hardas S, St R. Sultana, Clair DK, Vore M, Butterfield DA. Glutathione elevation by gamma-glutamyl cysteine ethyl ester as a potential therapeutic strategy for preventing oxidative stress in brain mediated by in vivo administration of adriamycin: implication for chemobrain. J. Neurosci. Res. 2007; 85:497–503. [PubMed: 17171703]

[57]. Oz M, Nurullahoglu Atalik KE, Yerlikaya FH, Demir EA. Curcumin alleviates cisplatin-induced learning and memory impairments. Neurobiol. Learn. Mem. 2015; 123:43–49. [PubMed: 25982942]

[58]. Pompella A, Visvikis A, Paolicchi A, Tata VD, Casini AF. The changing faces of glutathione, a cellular protagonist. Biochem. Pharmacol. 2003; 66:1499–1503. [PubMed: 14555227]

[59]. McLellan LI, Lewis AD, Hall DJ, Ansell JD, Wolf CR. Uptake and distribution of N-acetylcysteine in mice: tissue-specific effects on glutathione concentrations. Carcinogenesis. 1995; 16:2099–2106. [PubMed: 7554060]

[60]. Adair JC, Knoefel JE, Morgan N. Controlled trial of N-acetylcysteine for patients with probable Alzheimer's disease. Neurology. 2001; 57:1515–1517. [PubMed: 11673605]

[61]. Millea PJ. N-acetylcysteine: multiple clinical applications. Am. Fam. Physician. 2009; 80:265–269. [PubMed: 19621836]

[62]. Sandhir R, Sood A, Mehrotra A, Kamboj SS. N-Acetylcysteine reverses mitochondrial dysfunctions and behavioral abnormalities in 3-nitropropionic acid-induced Huntington's disease. Neurodegener. Dis. 2012; 9:145–157. [PubMed: 22327485]

[63]. Cascinu S, Catalano V, Cordella L, et al. Neuroprotective effect of reduced glutathione on oxaliplatin-based chemotherapy in advanced colorectal cancer: a randomized, double-blind, placebo-controlled trial. J. Clin. Oncol. 2002; 20:3478–3483. [PubMed: 12177109]

[64]. Estensen RD, Levy M, Klopp SJ, et al. N-Acetylcysteine suppression of the proliferative index in the colon of patients with previous adenomatous colonic polyps. Cancer Lett. 1999; 147:109–114. [PubMed: 10660096]

[65]. Holoye PY. Ifosfamide plus N-acetylcysteine in the treatment of small cell and non-small cell carcinoma of the lung: a Southeastern Cancer Study Group Trial. Cancer Treat. Rep. 1987; 71:431–432. [PubMed: 3030548]

[66]. Morgan LR, Donley PJ, Harrison EF, Hunter HL. Protective effect of N-acetylcysteine on the urotoxicity produced by oxazaphosphorine without interference with anticancer activity. Eur. J. Cancer Clin. Oncol. 1982; 18:113–114. [PubMed: 7200891]

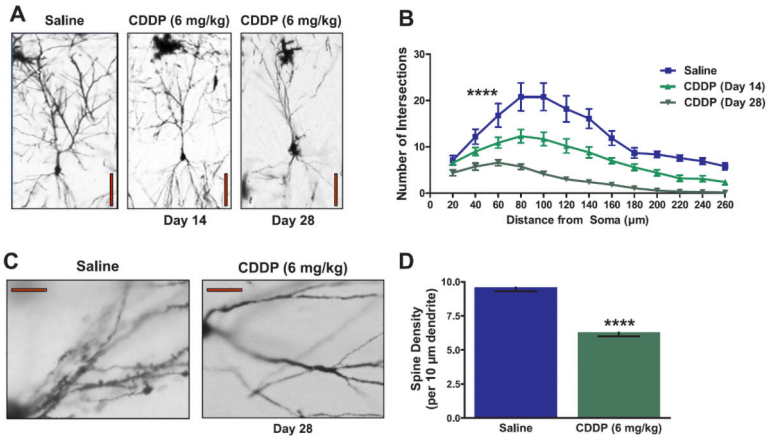

Fig. 1.

Acute CDDP treatment reduces hippocampal dendritic branching and spine density of pyramidal neurons at 14 and 28 days after treatment. (A) Representative Golgi-impregnated CA3 pyramidal neuron images and (B) graph illustrate the time-dependent reduction in dendritic branching caused by low-dose, 6 mg/kg CDDP. Compared to controls, CDDP treated rats have significantly less dendrite branch points from the soma of pyramidal neurons (n=6 rats per group, 2 neurons per rat). Scale bars, 40 μm. (C) Representative images and (D) graph of CA3 dendritic spines depicting significant reduction in spine density 28 days after CDDP exposure (n=24 dendritic branches per group). Data represented as mean ± SEM, **** $P < 0.0001$. Scale bars, 10 μm.

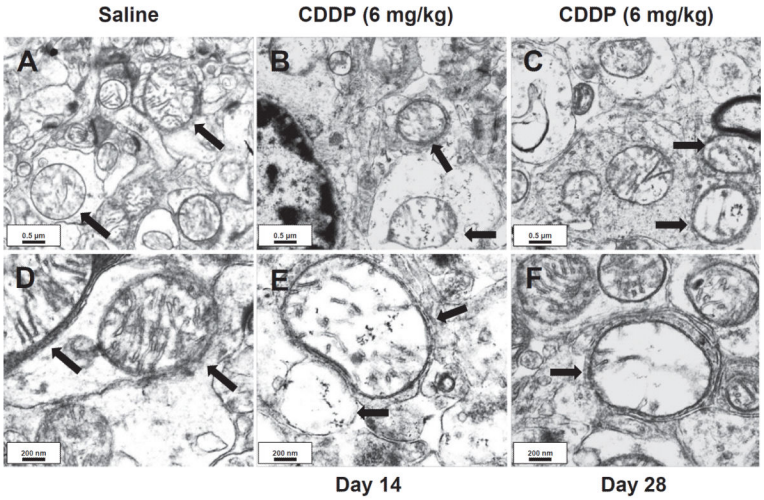

Fig. 2.

Acute CDDP treatment induces mitochondrial degradation and vacuolization in the rat hippocampus. Adult Sprague-Dawley rats were treated with CDDP (6 mg/kg) and hippocampal mitochondrial morphology was assessed at 14 and 28 days after treatment. (A, D) Representative EM images of CA3 neuronal mitochondria, with arrows showing intact normal mitochondria in control CA3 neurons. CDDP (6 mg/kg) induced mitochondrial vacuolization and degradation (arrows) (B, E) 14 days after treatment, with more extensive damage at (C, F) 28 days.

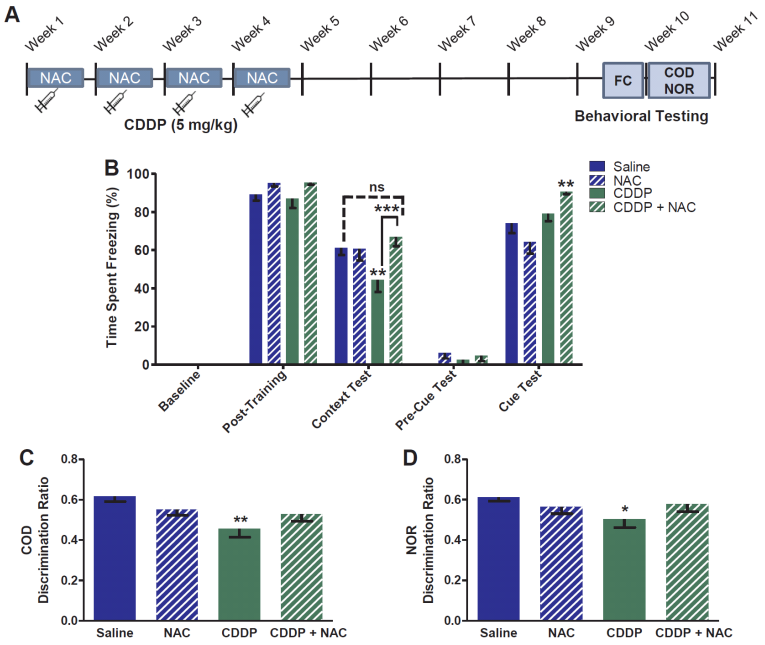

Fig. 3.

Chronic CDDP exposure impairs context discrimination memory and object recognition, which can be mitigated by NAC. (A) Study timeline. To recapitulate the clinical regimen, rats received one CDDP injection (5 mg/kg) per week for four consecutive weeks with or without NAC (250 mg/kg/day, i.p.). Rats were subjected to Fear Conditioning (FC) testing five weeks after the last CDDP injection, followed one week later by Context-Object Discrimination (COD) and Novel Object Recognition (NOR) Task. (B) CDDP significantly impaired performance on a contextual fear conditioning task. Baseline freezing levels were equivalent across all groups, and all groups showed increased freezing behavior, as expected, in response to a series of 5 tone-shock pairings (“Post-Training”). The context test was administered 24 h later, and CDDP-treated animals showed decreased freezing compared with the controls. NAC administration prevented the CDDP-induced deficit in the context test. The rats were placed in a novel context 1 h later for the cue test. There was no difference in freezing during the baseline or tone presentations, which indicated that CDDP did not disrupt the CS-US association. (C) The CDDP-treated rats had diminished ability to discriminate the out-of-context from the in-context object on the COD task. (D) Cisplatin-treated rats had reduced ability to discriminate between the novel and familiar objects on the NOR task. NAC administration partially ameliorated the CDDP-induced deficit in the COD and NOR tasks. Graphs represent mean ± SEM, Saline n=25, NAC n=18, CDDP n=15, CDDP+NAC n=13. *$P < 0.05$, **$P < 0.01$, ***$P < 0.001$, ns=not significant.

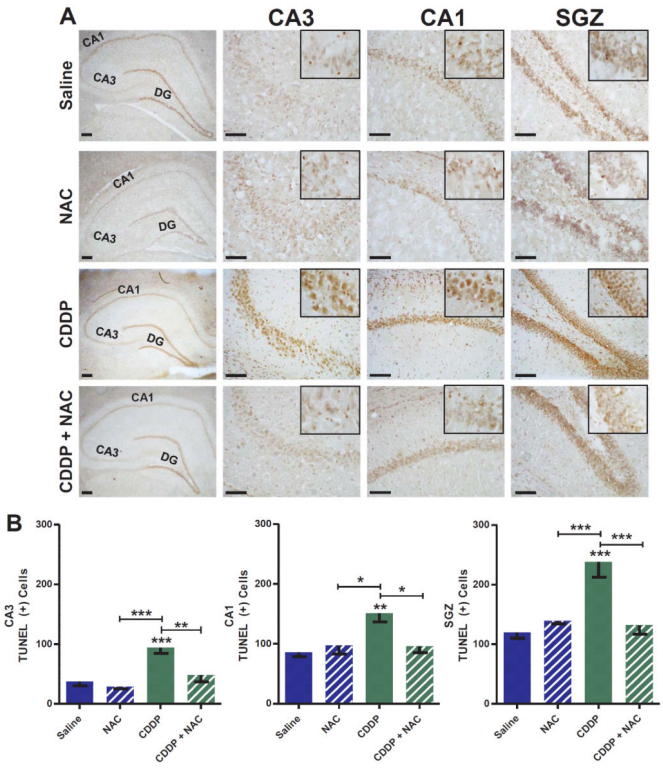

Fig. 4.

Chronic CDDP treatment increases TUNEL(+) cells in the rat hippocampus, NAC treatment attenuates apoptotic cell death. Adult Sprague-Dawley rats were treated with chronic CDDP regimen and neural apoptosis was assessed in the hippocampus after cognitive testing. (A) Representative images of hippocampal coronal sections show an increase in TUNEL(+) cells in the CA3, CA1, and SGZ of the DG after CDDP treatment, NAC significantly reduced CDDP-induced apoptotic cell death. Magnification used is 4× for the whole hippocampus, 20x for the other panels and 40× for the inserts. Scale bars: 4×, 200 μm; 20×, 100 μm. (B) Quantification of TUNEL(+) cells situated in the CA3 and CA1, and SGZ areas. Graphs represent mean ± SEM, n=2 subjects per treatment group, 4 replicates per subject. $*P < 0.05$, $** P < 0.01$, $***P < 0.001$.

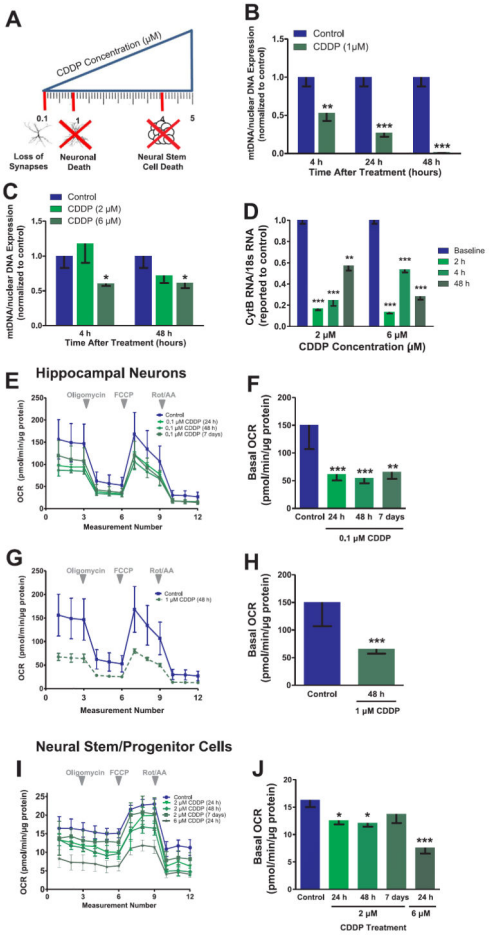

Fig. 5.

CDDP induces *mt*DNA breakage and mitochondrial respiratory dysfunction in cultured hippocampal neurons and NSCs. (A) Schematic representation of neuronal and NSC sensitivities to CDDP. Low-dose CDDP (0.1 μM) causes loss of synapses, while higher doses cause neuronal death (1 μM), followed by NSC death (4 μM). CDDP causes a severe decrease in (B) neuronal and (C) NSC *mt*DNA levels. qPCR demonstrates selective reduction in amplification of a *mt*DNA fragment (235 bp) compared to a nuclear gene (Clusterin) after CDDP treatment. (D) Decreased expression of mitochondrial encoded CytB after CDDP administration in NSCs. The ratio of CytB RNA and 18S rRNA was quantified by PCR and normalized to baseline levels. The Seahorse Bioscience XF24 was used to measure the Oxygen Consumption Rate (OCR). OCR is significantly decreased in cultured hippocampal neurons treated with CDDP at (E,F) 0.1 μM and (G,H) 1 μM. (F,H) Quantification of neuronal basal OCR levels. (I,J) CDDP treatment (2 μM, 6 μM) reduced mitochondrial respiratory rates in NSCs. (J) Quantification of NSC basal OCR levels. Graphs represent mean ± SEM of three biological replicates. * $P < 0.05$, ** $P < 0.01$, *** $P < 0.001$.

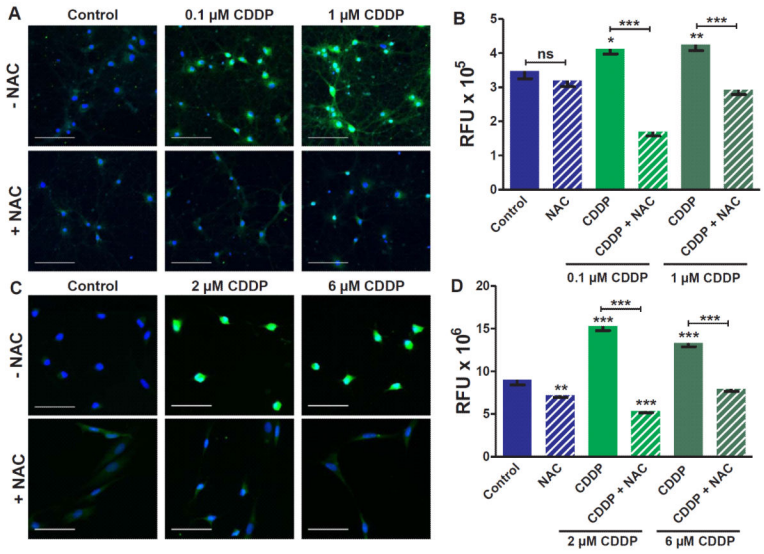

Fig. 6.

In-vitro, CDDP treatment increases oxidative stress in hippocampal neurons and NSCs, which can be attenuated by NAC treatment. (A) Rat hippocampal neurons (17 DIV) were exposed to 0.1 μM and 1 μM CDDP in presence or absence of NAC (2.5 mM) for 48 h. (B) Quantification of oxidative stress in CDDP and CDDP+NAC treated hippocampal neurons. (C) NSCs were exposed to 2 μM and 6 μM CDDP with or without NAC (5 mM) for 48 h. (D) Quantification of oxidative stress in CDDP and CDDP+NAC treated NSCs. Graphs represent mean ± SEM, three sister coverslips per treatment. 5 frames/coverslip. Scale bars, 100 μm. * $P < 0.05$, ** $P < 0.01$, *** $P < 0.001$, ns=not significant. (Blue, DAPI; Green, CellROX Oxidative Stress).

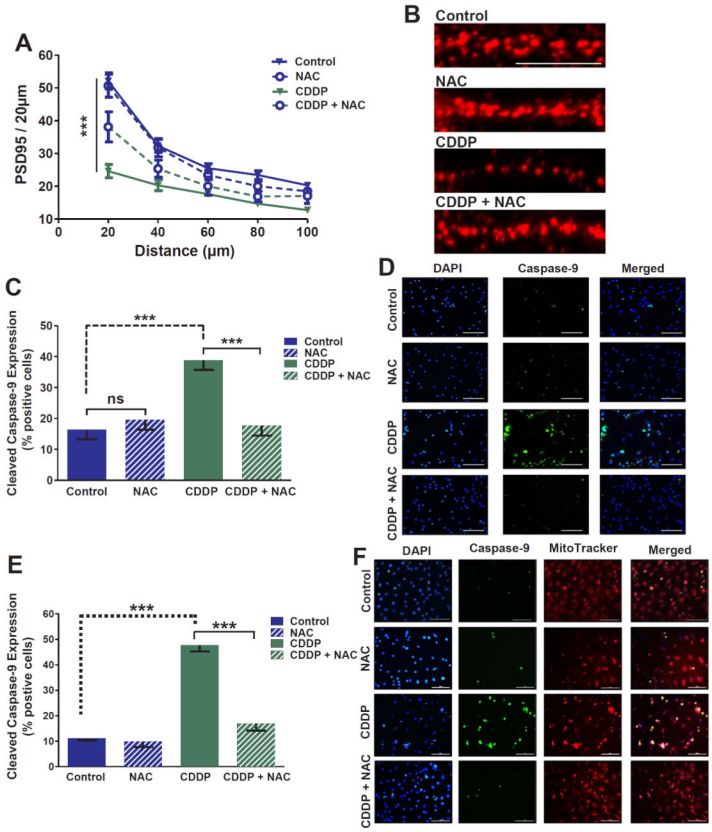

Fig. 7.

In-vitro, CDDP induces dendritic spine loss and apoptosis in hippocampal neurons and NSCs, which can be mitigated by NAC treatment. Rat hippocampal neurons (17 DIV) were exposed to 1 µM CDDP in presence or absence of NAC (2.5 mM) for 48 h. (A) Graph and (B) representative images of dendrites immuno-labeled for PSD95 depicting reduction in spine density after exposure to 1 µM CDDP. NAC treatment significantly reduced CDDP-induced spine-loss. Scale bars, 20 µm (C) Graph and (D) representative images of caspase-9 activation in hippocampal neurons following CDDP treatment. NAC significantly ameliorated CDDP-induced caspase-9 activation. Rat NSCs were exposed to 6 µM CDDP with or without NAC (5 mM) for 48 h. (E) Graph and (F) representative images of caspase-9 activation in NSCs following CDDP treatment. NAC significantly reduced caspase-9 activation in CDDP-treated NSCs. (blue, DAPI; green, caspase-9; red, PSD-95 (neurons); red, MitoTracker (NSCs). Graphs represent mean ± SEM of three sister coverslips per treatment. 5 frames/coverslip. Scale bars, 100 µm (ns=not significant, * $P < 0.05$, ** $P < 0.01$, *** $P < 0.001$).